Environmental influences over the last 16 ka on compound-specific $\delta^{13}C$ variations of leaf wax *n*-alkanes in the Hani peat deposit from northeast China

Shinya Yamamoto [a,] *, Kimitaka Kawamura [a], Osamu Seki [a], Philip A. Meyers [a, b], Yanhong Zheng [c], Weijian Zhou [d]

[a] Institute of Low Temperature Sciences, Hokkaido University, N19W8, Kita-ku, Sapporo 060-0819, Japan

[b] Department of Geological Sciences, The University of Michigan, Ann Arbor, Michigan, 48109-1005, U.S.A.

[c] State Key Laboratory of Continental Dynamics, Department of Geology, Northwest University, Xi'an, 710069, China

[d] State Key Laboratory of Loess and Quaternary Geology, Institute of Earth Environment, Chinese Academy of Sciences, Xi'an 710075, China

* Corresponding author. Tel: +81-11-706-5503; Fax: +81-11-706-7142

E-mail address: s.yamamoto@pop.lowtem.hokudai.ac.jp (S. Yamamoto)

Institute of Low Temperature Sciences, Hokkaido University, N19W8, Kita-ku, Sapporo 060-0819, Japan

Abstract

Compound-specific carbon isotope ratios ($\delta^{13}C$) of leaf wax *n*-alkanes (C_{21}-C_{33} odd carbon numbered *n*-alkanes) were measured in the Hani peat sequence from northeast China. These data were compared with lipid biomarker compositions to assess changes in local vegetation and paleoclimate for the last 16 ka. The $\delta^{13}C$ values of *n*-alkanes range between –36.6 to –30.7‰, showing that the compounds originate from C_3 plants. Much larger variations (~5.4‰) in the *n*-alkane $\delta^{13}C$ values than those of atmospheric CO_2 during the last 16 ka (< 0.5‰) indicate that the isotopic values were affected by environmental factors in addition to the postglacial $\delta^{13}C$ variations in the atmospheric reservoir. The stratigraphic records of $\delta^{13}C$ reveal decoupled fluctuations among the individual *n*-alkanes, particularly between 15.5 to 11.4 ka. Synchronous excursions in the $\delta^{13}C$ offsets among individual *n*-alkanes ($\Delta\delta^{13}C$) and lipid biomarker paleoplant proxies (P*aq*, and C_{23}/C_{31} and C_{27}/C_{31}) from 14.9 to 13.2 ka and 12.7 to 11.6 ka suggest that vegetational changes are the most likely causes for the decoupled $\delta^{13}C$ variations. Parallel fluctuations of the $\delta^{13}C$ values of terrestrial higher plant-derived C_{29} and C_{31} *n*-alkanes and the *n*-alkane average chain-length (ACL) from 11 to 6 ka indicate that the $\delta^{13}C$ variations responded to net evaporation changes. Negative shifts in the *n*-alkane $\delta^{13}C$ values coinciding with the ACL decreases at 10.5-9.3 ka and 8.1 ka indicate the short-term onset and fluctuations of the summer monsoon strength in eastern China during the early Holocene.

Keywords: peat; stable carbon isotopes; *n*-alkane; leaf wax; Holocene; Asian monsoon

1. Introduction

A peat deposit, which is an accumulation of partially decomposed and thermally immature organic matter that is mainly composed of autochthonous vascular plant debris, holds valuable information about continental paleoenvironmental histories

(Blackford, 2000). The kind and abundance of bog vegetation that contributes to a peat sequence can be significantly influenced by local factors such as bog surface moisture conditions, ground water level, influx of nutrient-rich groundwater, and lateral variety in plant communities, while regional climate changes can affect bog vegetation and its preservation in the peat sequence through the hydrology. Plant fossil records in the peat can therefore serve as a proxy for past climate changes (Barber, 1985). Indeed, various studies have reconstructed paleoenvironmental histories of peat bogs using pollen, plant macrofossils and the stable carbon and oxygen isotopic compositions of plant cellulose (Pendall et al., 2001; Hong et al., 2001; Xu et al., 2006; Schröder et al., 2007), as well as other proxies like humification indices (Blackford and Chambers, 1993; Baker et al., 1999; Wang et al., 2004) and testate amoebae (Charman, 2001).

Molecular compositions of lipid biomarkers derived from peat-forming plants have also been shown to be important proxies to reconstruct past changes in bog environments (Ficken et al., 1998; Nott et al., 2000; Pancost et al., 2002; Xie et al., 2004; Zhou et al., 2005; Zheng et al., 2007; López-Díaz et al., 2010). Records of peat *n*-alkanes are particularly robust because of their low susceptibility to microbial degradation relative to other types of lipid compound classes (Meyers, 2003; Zheng et al., 2007; Zhou et al., 2010), and their preferential production in the plant leaves rather than the roots (Pancost et al., 2002) make their stratiform depositional records preferable for paleoenvironmental archives, especially in a bog where plant macrofossils are sometimes poorly preserved.

Several studies have also employed compound-specific carbon isotopic analyses of *n*-alkanes to obtain additional paleoenvironmental information (Ficken et al., 1998; Xie et al., 2004). Because the individual leaf wax *n*-alkanes in a peat bog originate from a mixture of various types of vegetation with specific *n*-alkane distributions and carbon isotopic compositions ($\delta^{13}C$) (e.g. Corrigan et al., 1973; Ficken et al., 1998; Yudina and Savel'eva, 2008), a combination of *n*-alkane distributions and

76 their $\delta^{13}C$ values can make it possible to identify changes in the contributing plant
77 species. Furthermore, the $\delta^{13}C$ of terrestrial and peat-forming C_3 plants is partially
78 controlled by isotopic fractionations that reflect physiological responses to conditions in
79 their growing environment, such as humidity, temperature, and light level (Arens et al.,
80 2000; Hong et al., 2001). Thus, the leaf wax $\delta^{13}C$ values may also provide information
81 about the local paleoenvironment.
82 In the northeastern part of China, Holocene peat mires and lakes are widely
83 distributed, some of which have been intensively studied to reconstruct the Holocene
84 climate changes that were induced by variations in the Asian monsoon activity. For
85 example, paleoenvironmental proxies such as paleo-lake levels, pollen and
86 loess/paleosol records have revealed an increase in summer monsoon precipitation
87 during the last deglaciation and the early Holocene (An et al., 2000 and references
88 therein). Recently, the stable carbon and oxygen isotopic compositions of plant cellulose
89 (Hong et al., 2005, 2009a) and the molecular and hydrogen isotopic compositions of
90 lipid biomarkers (Seki et al., 2009; Zhou et al., 2010) have been examined in the Hani
91 peat deposit from northeastern China to reconstruct paleoclimatic history for the last 16
92 ka.
93 In this study, we present the $\delta^{13}C$ profiles of leaf wax *n*-alkanes in the Hani
94 peat sequence, and we use these profiles to reconstruct paleoenvironmental changes that
95 are recorded in the $\delta^{13}C$ of terrestrial higher plants. The combination of the $\delta^{13}C$ and
96 molecular distribution of *n*-alkanes allows us to estimate changes in source vegetation
97 and paleoclimatic history in northeastern China over the last 16 ka.
98
99 **2. Experimental**
100 **2.1. Setting and stratigraphy of the Hani peat deposit**
101 The Hani peat bog (42°13'N, 126°31'E) is located near Liangshui in Jilin
102 Province (Fig. 1) at an elevation of 900 m and is surrounded by the numerous volcano

cones and crater lakes that form the Long Gang volcanic field. The peat covers an area of 16.8 km^2 in a percolation mire where the Hani River has its source, and the stable swampy environment has allowed development of a peat layer more than 9 m thick since the end of the Last Glacial Maximum.

A core of the 963 cm thick peat sequence was recovered from near the center of the Hani bog. It is mainly composed of peat of various colors with occasional intercalations of mud and sand layers. The basal 33 cm of the core is marked with a dark gray mud layer, which is followed by a 204 cm-thick black-brown peat layer. The interval between 726 and 126 cm below the bog surface consists mainly of dark-brown peat. A mixed layer of light-brown peat with coarse sand and a layer of light-brown peat with abundant plant debris are intercalated at 640-606 and 316-246 cm depth intervals, respectively. The uppermost 126 cm interval near the surface is composed of 60 cm-thick brown peat and 40 cm-thick light-brown peat layers, in ascending order, which is capped with 26 cm of undegraded grass fragments (Fig. 2).

We developed an age-depth model based on calibrated calendar ages that were obtained from accelerator mass spectrometry (AMS) ^{14}C ages provided by Zhou et al. (2010) using CALIB 4.3 software (Stuiver and Reimer, 1993; Stuiver et al., 1998; Fig. 2). The peat accumulation rate averages 62 cm/ka, and the basal age of the entire 960 cm core sequence is 15.5 ka.

2.2. Lipid analyses

The samples consist of 1 cm sediment slices taken every 10 cm in the core. Lipids were ultrasonically extracted with $CHCl_3$ from ca. 1-2 g of freeze dried sample at the State Key Laboratory of Loess and Quaternary Geology in Xi'an, China. The extracts were concentrated on a rotary evaporator under vacuum and taken to dryness with a N_2 stream (Seki et al., 2009; Zhou et al., 2010). Aliphatic hydrocarbons were isolated using silica gel column chromatography (230-400 mesh; 1% H_2O deactivated)

130 by elution with 1.5 ml *n*-hexane at the Institute of Low Temperature Science, Hokkaido
131 University.
132 Analysis of aliphatic hydrocarbon fractions was performed using gas
133 chromatography (GC) and GC/mass spectrometry (MS). GC analysis was performed
134 using a Hewlett-Packard 6890 gas chromatograph equipped with an on-column injector,
135 CP-Sil 5 CB fused silica column (60 m × 0.32 mm i.d., 0.25 μm film thickness) and a
136 flame ionization detector (FID). Helium was used as carrier gas. The GC oven
137 temperature was programmed from 50 to 120˚C at 30˚C/min, from 120 to 310 °C at
138 6 °C/min, and then held isothermally for 15.5 min. GC/MS analysis was performed
139 using a Hewlett-Packard 5973 Mass Selective Detector coupled to a Hewlett-Packard
140 6890 gas chromatograph equipped with a HP-5MS fused silica column (30 m × 0.25
141 mm i.d., 0.25 μm film thickness). The temperature program was the same as for the GC
142 analysis. The compounds were identified on the basis of their mass spectra, GC
143 retention times, and comparison with literature mass spectra.
144
145 **2.3. Compound-specific stable carbon isotope analysis**
146 In order to improve the accuracy of the compound-specific stable carbon isotope
147 ratio ($\delta^{13}C$) analyses, the *n*-alkane fractions were purified using the urea adduct
148 technique of Yamamoto and Kawamura (2010). Briefly, a saturated solution of urea in
149 methanol was added to the hydrocarbon fraction dissolved in *n*-hexane/acetone (2:1)
150 and gently stirred overnight using a mechanical stirrer to complete the adduction. After
151 adduction, the solvent was removed from the urea precipitate, which was rinsed with
152 fresh solvent (*n*-hexane/acetone, 2:1) three times to remove non-adducted materials.
153 The urea crystals were dried under a N_2 stream and the *n*-alkanes were recovered in
154 *n*-hexane after dissolution of the crystals in water.
155 $^{13}C/^{12}C$ ratios of the purified *n*-alkanes were determined using a HP 6890 GC
156 coupled to a Finnigan MAT Delta Plus isotope ratio mass spectrometer via a Finnigan

157 MAT combustion furnace maintained at a temperature of 850 °C. The GC was equipped
158 with HP-5MS fused silica column (30 m × 0.32 mm i.d., 0.25 μm film thickness). The
159 GC oven was programmed from 50 to 120 °C at 30 °C/min, from 120 to 310 °C at
160 5 °C/min, and then held isothermally for 22 min. One to 2 μl of sample solution were
161 injected into the GC via an on-column injector with an internal standard of known
162 isotopic composition (C_{20} *n*-alkanoic acid methyl ester; $\delta^{13}C$ = –26.21‰). The $\delta^{13}C$
163 values are expressed as per mil (‰) relative to the Vienna Pee Dee Belemnite (VPDB).
164 Most measurements were duplicated. Reported $\delta^{13}C$ data represent an averaged value of
165 the duplicate analyses. An external standard consisting of C_{16} to C_{30} *n*-alkanes of known
166 isotopic compositions was daily injected into the GC/IRMS system to check the data
167 quality and to ensure that the analytical error of the *n*-alkanes remained below ±0.5‰
168 during the analyses (Bendle et al., 2007).
169
170 **3. Results and Discussion**
171 **3.1. $\delta^{13}C$ values of leaf wax *n*-alkanes in the Hani peat core**
172 The Hani peat core samples contain C_{21} to C_{35} *n*-alkanes with a strong
173 odd-over-even carbon number predominance (CPI = 3.1 to 7.5) as major aliphatic
174 hydrocarbons (Fig. 2). Generally, submerged and floating macrophytes contain a large
175 proportion of *n*-alkanes that maximizes at C_{21}, C_{23}, or C_{25}, whereas vascular land plants
176 and emersed macrophytes contain C_{27}, C_{29} and C_{31} *n*-alkanes as constituents of their
177 epicuticular waxes (e.g. Eglinton and Hamilton, 1967; Corrigan et al., 1973; Cranwell,
178 1984; Rieley et al., 1991; Ficken et al., 2000). Distribution patterns of these *n*-alkanes
179 show significant variations throughout the core (Fig. 2), suggesting variable
180 contributions from both types of plants.
181 Fig. 3 presents the profiles of the stable carbon isotopic compositions ($\delta^{13}C$)
182 of C_{21} to C_{33} odd carbon number *n*-alkanes in the Hani peat core. The $\delta^{13}C$ values of leaf
183 wax *n*-alkanes in the peat samples range from –36.6 to –30.7‰ (Fig. 3), which is in the

range of the $\delta^{13}C$ values reported for leaf wax *n*-alkanes in various Far East C_3 plants (Chikaraishi and Naraoka, 2003) and in surface soil samples from eastern China dominated by C_3 broad leaved forests (Rao et al., 2009). Inasmuch as cellulose $\delta^{13}C$ values have revealed that the contemporary vegetation in the Hani peat bog is dominated by C_3 plant species (Hong et al., 2005), the leaf waxes likely originate from the C_3 vegetation that flourished in the Hani peat bog. The $\delta^{13}C$ values of the leaf wax *n*-alkanes are, however, ca. 8‰ isotopically depleted in ^{13}C compared with those in the plant cellulose (Hong et al., 2005). Such depletion in leaf wax *n*-alkanes relative to peat cellulose reflects increased carbon isotopic fractionation between lipids and plant tissues in the acetate-malonate biosynthetic pathway (Collister et al., 1994).

The $\delta^{13}C$ of C_3 plants is partially controlled by the isotopic fractionations that are affected by various ecological and physiological factors and the species composition of their source vegetation (Arens et al., 2000), in addition to the isotopic composition of atmospheric CO_2. Much larger variations (~5.4‰) in leaf wax *n*-alkanes (Fig. 3) than those of atmospheric CO_2 during the last 16 ka (~0.5‰; Leuenberger et al., 1992) indicate that the $\delta^{13}C$ variations were mainly controlled by factors other than the postglacial $\delta^{13}C$ variations in the atmospheric reservoir.

3.2. Impact of vegetational changes on the $\delta^{13}C$ of leaf wax *n*-alkanes

Our records of the compound-specific $\delta^{13}C$ values show decoupled fluctuations among the individual *n*-alkanes (Fig. 3). In particular, the decoupling is prominent in the 960 to 650 cm interval where the $\delta^{13}C$ values of the C_{25} and C_{27} *n*-alkanes decrease to as low as –36.6‰ in contrast to the smaller fluctuations from –34.8 to –30.7‰ in the $\delta^{13}C$ values of the other *n*-alkanes (C_{21}, C_{23}, C_{29}, C_{31} and C_{33}) (Fig. 3). In the lower half of this interval (960 to 739 cm), the $\delta^{13}C$ profiles of the C_{23} and C_{25} *n*-alkanes exhibit a 2.0 to 2.5‰ negative shift, but equivalent shifts are not observed in the other *n*-alkane records. In the upper half of the interval (739 to 650 cm),

211 although C_{21} to C_{29} *n*-alkane profiles show concurrent $\delta^{13}C$ negative shifts, the
212 magnitudes of the shifts are significantly different among the compounds: those for C_{25}
213 and C_{27} are ca. 3.8‰, whereas those for the other *n*-alkanes are only 1.5 to 2.0‰ (Fig.
214 3).

215 The leaf wax *n*-alkanes in a peat bog are commonly derived from an
216 assemblage of different plants, each with specific *n*-alkane distributions and $\delta^{13}C$ values
217 (Ficken et al., 1998). Hence, the decoupling in the $\delta^{13}C$ variations of *n*-alkanes with
218 different chain-lengths may indicate that the $\delta^{13}C$ values of individual *n*-alkanes reflect
219 changes in plant community compositions that contribute to the peat *n*-alkanes. In
220 support of this idea, pollen records from Lake Sihailongwan, northeast China, have
221 revealed a gradual transition from steppe and open taiga-like woodland communities
222 during the late glacial to the earliest Holocene toward the dense deciduous forests that
223 are similar to modern flora (Schettler et al., 2006; Stebich et al., 2009). Similarly, the
224 ecophysiological responses to environment stresses may have been different among the
225 assemblage of peat-forming plants, which would further emphasize the $\delta^{13}C$ offsets
226 among individual compounds.

227 In this study, we assessed the possible impact of changes in the plant
228 communities on the $\delta^{13}C$ variations by comparison with the P*aq* and the concentration
229 ratios of the C_{21} to C_{33} odd carbon number *n*-alkanes against the C_{31} *n*-alkane. The P*aq*
230 (Ficken et al., 2000) is a paleoplant proxy expressed by the following equation:

231 $$Paq = (C_{23}+C_{25})/(C_{23}+C_{25}+C_{29}+C_{31})$$

232 that can reveal the proportion of aquatic (submerged and floating) macrophytes to total
233 peat forming plant taxa and has already been shown to be informative in the Hani peat
234 deposit (Seki et al., 2009; Zhou et al., 2010). The *n*-alkane ratios, especially the C_{27}/C_{31}
235 and C_{23}/C_{31} ratios are also known as paleoplant proxies. The C_{27}/C_{31} concentration ratio,
236 which was originally described as C_{31}/C_{27} ratio in Schwark et al. (2002), is generally
237 considered to express the relative contribution of C_3 grasses whose leaf wax *n*-alkanes

238 are dominated by the C_{31} homologue. However, the dominant *n*-alkane chain-lengths in
239 contemporary vegetation at the Hani peatland (Table 1) and the surrounding mountains
240 (Schröder et al., 2007; Makohonienko et al., 2008) from the literature suggest that the
241 C_{31} *n*-alkane may also be supplied to the peat deposit by some mosses and trees (e.g.
242 *Juglans*, *Betula, Abies, Taxus, Tilia, Fraxinus* and *Larix*) besides C_3 grasses. In contrast,
243 the C_{23}/C_{31} concentration ratio can represent the contribution of *Sphagnum* species
244 (Pancost et al., 2002). It is based on the observation that *Sphagnum* yields preferentially
245 C_{23} and C_{25} *n*-alkanes compared to other homologues (Ficken et al., 1998; Nott et al.,
246 2000; Pancost et al., 2002; Table 1).
247 In Fig. 4, we compare the profiles of the P*aq* and the *n*-alkane biomarker
248 ratios with those of the $\delta^{13}C$ offsets between the C_{31} *n*-alkane and the C_{21}, C_{23}, C_{25}, C_{27},
249 C_{29} and C_{33} *n*-alkanes; hereafter expressed as $\Delta\delta^{13}C$ ($C_{31} - C_{21}$), $\Delta\delta^{13}C$ ($C_{31} - C_{23}$), $\Delta\delta^{13}C$
250 ($C_{31} - C_{25}$), $\Delta\delta^{13}C$ ($C_{31} - C_{27}$), $\Delta\delta^{13}C$ ($C_{31} - C_{29}$) and $\Delta\delta^{13}C$ ($C_{31} - C_{33}$), respectively. The
251 $\Delta\delta^{13}C$ records reveal significant positive excursions from 14.9 to 13.2 ka and 12.7 to
252 11.6 ka, although the magnitudes of the excursions of $\Delta\delta^{13}C$ ($C_{31} - C_{21}$), $\Delta\delta^{13}C$ ($C_{31} -$
253 C_{29}) and $\Delta\delta^{13}C$ ($C_{31} - C_{33}$) are much smaller than those of $\Delta\delta^{13}C$ ($C_{31} - C_{23}$), $\Delta\delta^{13}C$ (C_{31}
254 $- C_{25}$) and $\Delta\delta^{13}C$ ($C_{31} - C_{27}$) (Figs. 4a, b). The simultaneous changes in paleoplant
255 proxies with the excursions strongly suggest that vegetational changes are the most
256 likely causes for the decoupled variations among the *n*-alkane homologues. Changes in
257 the sedimentary environment may also have potentially affected the $\delta^{13}C$ values through
258 the enhancement of allochthonous plant input from the surrounding forests. However, a
259 lack of any clear relation between the $\delta^{13}C$ variations and the peat lithology suggests
260 that such an increase is unlikely.
261
262 *3.2.1. Vegetational change from 14.9 to 13.2 ka*
263 Parallel increases in the C_{23}/C_{31} ratios and the $\Delta\delta^{13}C$ ($C_{31} - C_{23}$), $\Delta\delta^{13}C$ ($C_{31} -$
264 C_{25}), $\Delta\delta^{13}C$ ($C_{31} - C_{27}$) and $\Delta\delta^{13}C$ ($C_{31} - C_{29}$) values from 14.9 to 13.2 ka (Figs. 4a-4c)

265 indicate that a relative increase in the contribution of *Sphagnum* species to the peat
266 *n*-alkanes is the most likely cause for the $\Delta\delta^{13}C$ increases in this period. This notion is
267 supported by the significant increases in the relative abundance of C_{21} and C_{25} *n*-alkanes
268 against the C_{31} *n*-alkane (Fig. 4c), because these homologues are predominantly found
269 in *Sphagnum* species (Ficken et al., 1998; Nott et al., 2000). Furthermore, the
270 magnitudes of the $\delta^{13}C$ offsets from the C_{31} *n*-alkane are ~ 3.4‰ for the C_{25} *n*-alkane
271 and ~ 3.8‰ for the C_{27} *n*-alkane, which match well with those observed in modern
272 *Sphagnum* species in which the $\delta^{13}C$ of the C_{25} and C_{27} *n*-alkanes are ~ 3.4‰ more
273 ^{13}C-depleted than the C_{31} *n*-alkane (Ficken et al., 1998). The potential contribution from
274 submerged/floating aquatic plants other than *Sphagnum* could have increased because
275 the C_{23} *n*-alkane is also abundant in these aquatic macrophytes (Ficken et al., 2000; Nott
276 et al., 2000). However, such vegetational changes are not supported by macrofossil
277 evidence from the Hani peat sequence (Schröder et al., 2007).
278 On the other hand, the pollen proxy record in nearby Lake Sihailongwan
279 revealed an increased influx from *Betula* between 14.3 to 14.0 ka (Stebich et al., 2009).
280 Because the C_{27} *n*-alkane is commonly found in *Betula* and *Fagus* trees (Table 1; Ali et
281 al., 2005; Sachse et al., 2006), parallel increases in the C_{27}/C_{31} and the $\Delta\delta^{13}C$ ($C_{31} - C_{27}$)
282 from 14.4 to 14.1 ka (Fig. 4) might correspond to climate amelioration at the beginning
283 of the Late Glacial.
284 Relatively high P*aq* values and D-depleted hydrogen isotopic compositions of
285 the *n*-alkanes during 14 to 11 ka (Seki et al., 2009; Fig. 4) indicate that the increases in
286 aquatic plants likely are the consequence of enhanced water availability for the
287 peat-forming plants. In percolation mires like the Hani sequence, rainwater generally
288 flows over the peat surface and infiltrates the peat body during the wet growing season
289 due to the slope of the peat surface and the large amount of precipitation in the summer.
290 However, macrofossil records from the Hani mire suggest that the establishment of the
291 initial stage of percolation conditions did not occur until at least 12.6 ka (Schröder et al.,

292 2007). Hence, the water availability is likely to have been controlled by groundwater
293 level during this period although a marked rise in the total pollen concentrations and
294 increases in frequencies of moss and fern spores and the accumulation rate of biogenic
295 silica in nearby lake Sihailongwan suggest an increased precipitation during 14.5 to
296 13.6 ka (Stebich et al., 2007, 2009).
297
298 *3.2.2. Vegetational change from 12.7 to 11.6 ka*
299 Simultaneous increases in $\Delta\delta^{13}C$ ($C_{31} - C_{27}$) values and C_{27}/C_{31} ratios from
300 12.7 to 11.6 ka (Figs. 4b, d) indicate a relative increase of ^{13}C-depleted C_{27} *n*-alkanes
301 and/or a relative decrease of ^{13}C-depleted C_{31} *n*-alkanes during this time interval.
302 Because a certain *Sphagnum* species, *Sphagnum fuscum*, is known to have a large
303 abundance of the C_{27} *n*-alkane (Corrigan et al., 1973; Sachse et al., 2006; Yudina and
304 Savel'eva, 2008) and to contain C_{23}, C_{25} and C_{27} *n*-alkanes whose $\delta^{13}C$ are 1.3 to 2.0‰
305 lower than those of the C_{29} and C_{31} *n*-alkanes (Ficken et al., 1998; Xie et al., 2004), the
306 increased contribution of this species can consistently explain the high C_{27}/C_{31} ratios and
307 the increase in the $\Delta\delta^{13}C$ ($C_{31} - C_{23}$), $\Delta\delta^{13}C$ ($C_{31} - C_{25}$) and $\Delta\delta^{13}C$ ($C_{31} - C_{27}$) values
308 during the 12.7 to 11.6 ka period (Figs. 4a, b). The lack of change in the C_{23}/C_{31} ratios
309 suggests that the contribution of *Sphagnum* mosses did not increase, unlike the period
310 from 14.9 to 13.2 ka; however, it should be noted that the C_{23}/C_{31} ratio does not always
311 indicate an abundant *Sphagnum* contribution to peat deposits when the predominant
312 *Sphagnum* species possesses both the C_{27} and C_{31} *n*-alkanes as its major components
313 (Nott et al., 2000).
314 On the other hand, pollen records in nearby Lake Shihailongwan show
315 increases in the relative abundance of certain conifers (*Larix*, *Picea*) during the period
316 of Younger Dryas-like climate deterioration (12.4-11.7 ka; Stebich et al., 2007, 2009).
317 Because the leaf wax of these conifer trees contains the C_{31} *n*-alkane with a more
318 ^{13}C-enriched $\delta^{13}C$ value than the C_3 angiosperms (Chikaraishi and Naraoka, 2003;

Maffei et al., 2004; Pedentchouk et al., 2008), the high C_{27}/C_{31} and $\Delta\delta^{13}C$ values (Fig. 4) could be consequences of a relative decrease in the proportions of ^{13}C-depleted C_{31} *n*-alkanes due to increases in conifer contributions.

3.3. Climate changes in northeastern China recorded in the $\delta^{13}C$ of plant leaf waxes

Paleoclimate changes in northeast China for the last 16 ka are characterized by a sequence of moisture changes. Various proxies document a general humidity increase during the Late-glacial period with three short-term climate reversals to cool and dry conditions at 13.9, 13.0 and 12.7 to 11.7 ka. In contrast, climate conditions in the Holocene were relatively dry as compared to the deglacial period, however, the summer monsoon rainfall record exhibits century-scale variability with maxima around 9.8 and 7.8 ka (An et al., 2000; Schettler et al., 2006; Stebich et al., 2007; Seki et al., 2009; Zhou et al., 2010).

In Fig. 5, we compare the fluctuations of the $\delta^{13}C$ of terrestrial higher plant *n*-alkanes (C_{29} and C_{31} *n*-alkanes) with those of the *n*-alkane averaged chain-length (ACL) and the oxygen isotope compositions ($\delta^{18}O$) of Hani peat cellulose (Hong et al., 2009a) in order to evaluate the influence of the paleoclimate changes on the $\delta^{13}C$ variations. The ACL value is the concentration-weighted mean chain-length of the C_{27}, C_{29} and C_{31} *n*-alkanes (Poynter et al., 1989), and its variations are commonly related to changes in the temperature and aridity of the growing environment of alkane source vegetation (Poynter et al., 1989; Kawamura et al., 2003; Schefuß et al., 2003; Rommerskirchen et al., 2003). More recently, Sachse et al. (2006) reported a correlation between the ACL and the hydrogen isotopic fractionation of leaf wax *n*-alkanes that suggests that plants can alter the chain-lengths of their leaf waxes to minimize evaporation of water vapor from their leaves. On the other hand, the cellulose $\delta^{18}O$ are considered to reflect changes in surface air temperature (Hong et al., 2009a, b).

346 The ACL shows concomitant variations with the cellulose $\delta^{18}O$ (Fig. 5),
347 suggesting that the variations, in part, likely reflect plant physiological responses to
348 changes in temperature-driven evaporation. In contrast, the $\delta^{13}C$ of terrestrial higher
349 plant *n*-alkanes (C_{29} and C_{31} *n*-alkanes) exhibit fluctuations that are concurrent with the
350 ACL and $\delta^{18}O$ variations from 11.2 to 6.5 ka (light gray band in Fig. 5).
351 Stable carbon-isotopic fractionation (εp) of terrestrial higher plants is often
352 expressed as the following equation (Farquhar et al., 1982):
353 $\varepsilon p = a + (b - a)\, Ci/\, Ca$
354 where Ci/Ca is the ratio of CO_2 concentration in the intercellular space of leaves (Ci) to
355 that in the atmosphere (Ca); a is the fractionation associated with diffusion of CO_2 from
356 the atmosphere into the intercellular space of leaves (4.4‰) and b is the fractionation of
357 CO_2 during carboxylation mediated by Rubisco (ca. 30‰). With higher evaporation
358 rates, plants would have reduced stomatal conductance to minimize the evaporative loss
359 of water from their leaves and thereby lowering Ci/Ca, which results in the $\delta^{13}C$ of the
360 plants becoming more ^{13}C enriched, and vice versa. Hence, the concurrent fluctuations
361 between the $\delta^{13}C$ and the ACL values during the early Holocene indicate that the $\delta^{13}C$
362 variations reflect plant physiological responses to changes in net evaporation in Hani
363 region during the early Holocene.
364 Nevertheless, it should be noted that the $\delta^{13}C$ variations of terrestrial higher
365 plant *n*-alkanes (C_{29} and C_{31} *n*-alkanes) do not match with the ACL variations in the 15.5
366 to 11.4 ka and 6.5 to 0.1 ka intervals (Fig. 5). This absence of agreement could be partly
367 related to the origin of the *n*-alkanes, because the C_{29} and C_{31} *n*-alkanes can also be
368 produced by several mosses found in the Hani peatland (Table 1) besides terrestrial
369 higher plant leaf waxes. Isotopic fractionation during carbon fixation in mosses is
370 generally smaller than in other peat-forming plants due to the lack of functional stomata
371 and a waxy cuticle on the leaf epidermis (Xie et al., 2004), and thus potential increases
372 in *n*-alkane inputs from mosses during wetter periods in the Late Glacial and in late

373 Holocene may conceal the $\delta^{13}C$ signals recorded in the *n*-alkanes derived from
374 evaporation-sensitive terrestrial higher plant.
375 Several lines of evidence indicate short-term enhancement of summer
376 monsoon rainfall in eastern China during the early Holocene. Wang et al. (1999)
377 examined the $\delta^{18}O$ of planktonic foraminifera in South China Sea sediments and
378 concluded that monsoon runoff and precipitation increased at ca. 9.4 and 8–8.1 ka in
379 southeast China. Nearly simultaneously, the net accumulation rate of biogenic silica
380 decreased (Schettler et al., 2006) and the $\delta^{13}C$ values of peat cellulose (Hong et al.,
381 2005) increased at 9.5 and 8.0 ka in northeast China (Fig. 5d), indicating an enhanced
382 summer monsoon rainfall at that time. Our *n*-alkane $\delta^{13}C$ records of terrestrial higher
383 plant *n*-alkanes (C_{29} and C_{31} *n*-alkanes) exhibit 1.4 to 1.8‰ negative shifts with the ACL
384 increases at 10.5–9.3 ka and 8.1 ka (dark gray bands in Fig. 5), which is likely to
385 represent the $\delta^{13}C$ responses of peat-forming terrestrial higher plant to the increases in
386 summer monsoonal precipitation in eastern China.
387 In northeast China, seasonal and inter-annual changes in temperature and
388 precipitation are connected with activity of the summer and winter monsoon. Most of
389 the annual precipitation is derived from the summer monsoon, and the distribution of
390 annual precipitation shows a gradual decrease toward the north-west. These
391 spatiotemporal patterns in monsoonal precipitation indicate that the short-term onset
392 and fluctuations of the summer monsoon strength may have significantly influenced the
393 early Holocene variations in effective precipitation in the Hani region.
394
395 **4. Summary and conclusions**
396 Compound-specific $\delta^{13}C$ values of C_{21} to C_{33} odd carbon number *n*-alkanes
397 (–36.6 to –30.7‰) were measured in the Hani peat deposit from northeast China to
398 assess possible changes in source vegetation and to reconstruct the regional
399 paleoclimatic history over the last 16 ka. Major changes were found in the isotopic and

400 molecular compositions of *n*-alkanes and are interpreted as follows.

401 1. The $\delta^{13}C$ profiles of individual *n*-alkanes show decoupled fluctuation
402 patterns particularly in the 960 to 650 cm interval (15.5 to 11.4 ka). A comparison
403 between the $\delta^{13}C$ offsets among individual *n*-alkane records ($\Delta\delta^{13}C$) and biomarker
404 paleoplant proxies (P*aq*, C_{23}/C_{31}, and C_{27}/C_{31}) reveal concurrent increases in C_{23}/C_{31}
405 ratios and $\Delta\delta^{13}C$ values from 14.9 to 13.2 ka that were most likely a result of enhanced
406 flourishing of *Sphagnum* plants (moss) during this time interval.

407 2. Larger C_{27}/C_{31} ratios and increases in $\Delta\delta^{13}C$ ($C_{31} - C_{27}$) and $\Delta\delta^{13}C$ ($C_{31} -$
408 C_{25}) occur in peat deposited from 12.7–11.6 ka. These changes are likely a consequence
409 of an increased relative contribution of ^{13}C-depleted C_{27}-dominated *Sphagnum* species
410 and/or a decreased contribution of ^{13}C-depleted C_{31} *n*-alkane due to the expansion of
411 conifers.

412 3. Parallel fluctuations between the $\delta^{13}C$ values of terrestrial higher
413 plant-derived *n*-alkanes (C_{29} and C_{31}) and the *n*-alkane average chain-length (ACL)
414 values during the early Holocene suggest that the $\delta^{13}C$ variation most likely reflect plant
415 physiological responses to changes in effective precipitation (i.e., precipitation minus
416 evaporation).

417 4. The $\delta^{13}C$ variations exhibit 1.4 to 1.8‰ negative shifts at 10.5–9.3 ka and
418 8.1 ka along with decreased ACL values, indicating that the effective precipitation in
419 northeastern China was variable during the early Holocene, probably due to short-term
420 enhancement of summer monsoon rainfall at that time.

421

422 **Acknowledgments**

423 We thank the two anonymous reviewers for their thoughtful comments, which
424 helped to improve this paper. This study was partly supported by the Japan Society for
425 the Promotion of Science (grant-in-aid 19204055), the National Science Foundation of
426 China, the Knowledge Innovation Program of the Chinese Academy of Science, and the

National Basic Research Program of China. S.Y. and P.A.M. gratefully acknowledge financial support from the Institute of Low Temperature Science, Hokkaido University.

429 **References**

430 Ali, H. A. M., Mayes, R. W., Hector, B. L., Verma, A. K., Ørskov, E. R., 2005. The
431 possible use of n-alkanes, long-chain fatty alcohols and long-chain fatty acids
432 as markers in studies of the botanical composition of the diet of free-ranging
433 herbivores. Journal of Agricultural Science 143, 85–95.

434 Arens, N. C., Jahren, A. H., Amundson, R., 2000. Can C3 plants faithfully record the
435 carbon isotopic composition of atmospheric carbon dioxide? Paleobiology 26,
436 137–164.

437 An, Z., Porter, S. C., Kutzbach, J. E., Wu, X., Wang, S., Liu, X., Li, Z., Zhou, W., 2000.
438 Asynchronous Holocene optimum of the East Asian monsoon. Quaternary
439 Science Reviews 19, 743–762.

440 Baas, M., Pancost, R., van Geel, B., Sinninghe Damsté, J. S., 2000. A comparative study
441 of lipids in *Sphagnum* species. Organic Geochemistry 31, 535–541.

442 Baker, A., Caseldine, C. J., Gilmour, M. A., Charman, D., Proctor, C. J., Hawkesworth,
443 C. J., Pillips, N., 1999. Stalagmite luminescence and peat humification records
444 of palaeomoisture for the last 2500 years. Earth and Planetary Science Letters
445 165, 157–162.

446 Barber, K. E., 1985. Peat stratigraphy and climatic change: Some speculations. In:
447 Tooley, M. J., Sheail, G. M. (Eds.), The Climatic Scene: Essays in Honour of
448 Gordon Manley. Allen and Unwin, London. pp. 175–185.

449 Bendle, J., Kawamura, K., Yamazaki, K., Niwai, T., 2007. Latitudinal distribution of
450 terrestrial lipid biomarkers and *n*-alkane compound-specific stable carbon
451 isotope ratios in the atmosphere over the western Pacific and Southern Ocean.
452 Geochimica et Cosmochimica Acta 71, 5934–5955.

453 Blackford, J. J., 2000. Paleoclimate records from peat. Trends in Ecology & Evolution
454 15, 193–195.

455 Blackford, J. J., Chambers, F. M., 1993. Determining the degree of peat decomposition

456 in peat-based palaeoclimatic studies. International Peat Journal 5, 7–24.
457 Charman, D. J., 2001. Biostratigraphic and Palaeoenvironmental applications of testate
458 amoebae. Quaternary Science Reviews 20, 1753–1764.
459 Chikaraishi, Y., Naraoka, H., 2003. Compound-specific δD-δ^{13}C analyses of n-alkanes
460 extracted from terrestrial and aquatic plants. Phytochemistry 63, 361–371.
461 Collister, J. W., Rieley, G., Stern, B., Eglington, G., Fry, B., 1994. Compound-specific
462 δ^{13}C analyses of leaf lipids from plants with differing carbon dioxide
463 metabolisms. Organic Geochemistry 21, 619–627.
464 Corrigan, D., Kloos, C., O'Connor, C. S., Timoney, R. F., 1973. Alkanes from four
465 species of *Sphagnum* moss. Phytochemistry 12, 213–214.
466 Cranwell, P. A., 1984. Lipid geochemistry of sediments from Upton Broad, a small
467 productive lake. Organic Geochemistry. 7, 25–37.
468 Eglinton, G., Hamilton, R. J., 1967. Leaf epicuticular waxes. Science 156, 1322–1335.
469 Farquhar, G. D., O'leary, M. H., Berry, J. A., 1982. On the relationship between carbon
470 isotope discrimination and the intercellular carbon dioxide concentration in
471 leaves. Australian Journal of Plant Physiology 9, 121–137.
472 Ficken, K. J., Barber, K. E., Eglinton, G., 1998. Lipid biomarker, δ^{13}C and plant
473 macrofossil stratigraphy of a Scottish montane peat bog over the last two
474 millennia. Organic Geochemistry 28, 217–237.
475 Ficken, K. J., Li, B., Swain, D. L., Eglinton, G., 2000. An *n*-alkane proxy for the
476 sedimentary input of submerged/floating freshwater aquatic macrophytes.
477 Organic Geochemistry 31, 745–749.
478 Hong, Y. T., Wang, Z. G., Jiang, H. B., Lin, Q. H., Hong, B., Zhu, Y. X., Wang, Y., Xu,
479 L. S., Leng, X. T., Li, H. D., 2001. A 6000-year record of changes in drought
480 and precipitation in northeastern China based on a δ^{13}C time series from peat
481 cellulose. Earth and Planetary Science Letters 185, 111–119.
482 Hong, Y. T., Hong, B., Lin, Q. H., Shibata, Y., Hirota, M., Zhu, Y. X., Leng, X. T., Wang,

Y., Wang, H., Yi, L., 2005. Inverse phase oscillations between the East Asian and Indian Ocean summer monsoons during the last 12000 years and paleo-El Niño. Earth and Planetary Science Letters 231, 337–346.

Hong, B., Liu, C. Q., Lin, Q. H., Shibata, Y., Leng, X. T., Wang, Y., Zhu, Y. X., Hong, Y. T., 2009a. Temperature evolution from the $\delta^{18}O$ record of Hani peat, Northeast China, in the last 14000 years. Science in China Series D: Earth Sciences 52, 952–964.

Hong, Y. T., Hong, B., Lin, Q. H., Shibata, Y., Zhu, Y. X., Leng, X. T., Wang, Y., 2009b. Synchronous climate anomalies in the western North Pacific and North Atlantic regions during the last 14,000 years. Quaternary Science Reviews 28, 840–849.

Kawamura, K., Ishimura, Y., Yamazaki, K., 2003. Four years' observations of terrestrial lipid class compounds in marine aerosols from the western North Pacific. Global Biogeochemical Cycles 17, 1003.

Leuenberger, M., Siegenthaler, U., Langway, C. C., 1992. Carbon isotope composition of atmospheric CO_2 during the last ice age from an Antarctic ice core. Nature 357, 488–490.

López-Díaz, V., Borrego, Á.G., Blanco, C.G., Aboleya, M., López-Sáez, J.A., López-Merino, L., 2010. Biomarkers in a peat deposit in Northern Spain (Huelga de Bayas, Asturias) as a proxy for climate variation. Journal of Chromatography A 1217, 3538–3546.

Maffei, M., Badino, S., Bossi, S., 2004. Chemotaxonomic significance of leaf wax *n*-alkanes in the Pinales (Coniferales). Journal of Biological Research 1, 3–19.

Meyers, P. A., 2003. Applications of organic geochemistry to paleolimnological reconstructions: a summary of examples from the Laurentian Great Lakes. Organic Geochemistry 34, 261–289.

Makohonienko, M., Kitagawa, H., Fujiki, T., Liu, X., Yasuda, Y., Yin, H., 2008. Late

510 Holocene vegetation changes and human impact in the Changbai Mountains
511 area, Northeast China. Quaternary International 184, 94–108.
512 Nichols, J., Booth, R. K., Jackson, S. T., Pendall, E. G., Huang, Y., 2006.
513 Paleohydrologic reconstruction based on *n*-alkane distributions in
514 ombrotrophic peat. Organic Geochemistry 37, 1505–1513.
515 Nott, C. J., Xie, S., Avsejs, L. A., Maddy, D., Chambers, F. M., Evershed, R. P., 2000.
516 *n*-Alkane distributions in ombrotrophic mires as indicators of vegetation
517 change related to climatic variation. Organic Geochemistry 31, 231–235.
518 Pancost, R. D., Baas, M., van Geel, B., Sinninghe Damsté, J. S., 2002. Biomarkers as
519 proxies for plant inputs to peats: an example from a sub-boreal ombrotrophic
520 bog. Organic Geochemistry 33, 675–690.
521 Pedentchouk, N., Sumner, W., Tipple, B., Pagani, M., 2008. $\delta^{13}C$ and δD compositions
522 of *n*-alkanes from modern angiosperms and conifers: An experimental set up
523 in central Washington State, USA. Organic Geochemistry 39, 1066–1071.
524 Pendall, E., Markgraf, V., White, J.W.C., Dreier, M., Kenny, R., 2001. Multiproxy
525 record of Late Pleistocene-Holocene climate and vegetation changes from a
526 peat bog in Patagonia. Quaternary Research 55, 168–178.
527 Poynter, J. G., Farrimond, P., Robinson, N., Eglinton, G., 1989. Aeolian-derived higher
528 plant lipids in the marine sedimentary record: links with palaeoclimate. In:
529 Leinen, M., Sarnthein, M. (Eds.) Paleoclimatology and paleometeorology:
530 modern and past patterns of global atmospheric transport. Kluwer Academic
531 Publishers, Dordrecht, The Netherlands. pp. 435–462.
532 Rao, Z., Zhu, Z., Jia, G., Henderson, A. C. G., Xue, Q., Wang, S., 2009. Compound
533 specific δD values of long chain *n*-alkanes derived from terrestrial higher
534 plants are indicative of the δD of meteoric waters: Evidence from surface soils
535 in eastern China. Organic Geochemistry 40, 922–930.
536 Rieley, G., Collier, R. J., Jones, D. M., Eglinton, G., Eakin, P. A., Fallick, A. E., 1991.

537 Sources of sedimentary lipids deduced from stable carbon-isotope analyses of
538 individual compounds. Nature 352, 425–427.
539 Rommerskirchen, F., Eglington, G., Dupont, L., Günter, U., Wenzel, C., Rullkötter, J.,
540 2003. A north to south transect of Holocene southeast Atlantic continental
541 margin sediments: Relationship between aerosol transport and
542 compound-specific $\delta^{13}C$ land plant biomarker and pollen records.
543 Geochemistry, Geophysics, Geosystems 4(12), 1101.
544 Sachse, D., Radke, J., Gleixner, G., 2006. δD values of individual *n*-alkanes from
545 terrestrial plants along a climatic gradient – Implications for the sedimentary
546 biomarker record. Organic Geochemistry 37, 469–483.
547 Schefuβ, E., Ratmeyer, V., Stuut, J.-B. W., Jansen, J. H. F., Sinninghe Damsté, J. S.,
548 2003. Carbon isotope analysis of *n*-alkanes in dust from the lower atmosphere
549 over the central eastern Atlantic. Geochimica et Cosmochimica Acta 67,
550 1757–1767.
551 Schettler, G., Liu, Q., Mingram, J., Stebich, M., Dulski, P., 2006. East-Asian monsoon
552 variability between 15000 and 2000 cal. yr BP recorded in varved sediments of
553 Lake Sihailongwan (northeastern China, Long Gang volcanic field). The
554 Holocene 16, 1043–1057.
555 Schröder, C., Thiele, A., Wang, S, Bu, Z., Joosten, H., 2007. Hani-mire – A percolation
556 mire in northeast China. Peatlands International 2, 21–24.
557 Schwark, L., Zink, K., Lechterbeck, J., 2002. Reconstruction of postglacial to early
558 Holocene vegetation history in terrestrial Central Europe via cuticular lipid
559 biomarkers and pollen records from lake sediments. Geology 30, 463–466.
560 Seki, O., Meyers, P. A., Kawamura, K., Zheng, Y., Zhou, W., 2009. Hydrogen isotopic
561 ratios of plant-wax *n*-alkanes in a peat bog deposited in northeast china during
562 the last 16kyr. Organic Geochemistry 40, 671–677.
563 Stebich, M., Arlt, J., Mingram, J., 2007. Late Quaternary vegetation history of N. E.

564 China – recent progress in the investigation of Sihailongwang maar lake. In:
565 Kahlke, R.-D. Maul, L. C., Mazza, P. (Eds.), Late Neogene and Quaternary
566 biodiversity and evolution: regional developments and interregional
567 correlations (Proceedings of the 18th international Senckenberg Conference
568 (VI International Palaeontological Colloquium in Weimar)). Courier
569 Forschungsinstitut Senckenberg 259, Stuttgart. pp. 181–190.
570 Stebich, M., Mingram, J., Han, J., Liu, J., 2009. Late Pleistocene spread of
571 (cool-)temperate forests in Northeast China and climate changes synchronous
572 with the North Atlantic region. Global and Planetary Change 65, 56–70.
573 Stuiver, M., Reimeer, P.J., 1993. Extended ^{14}C database and revised Calib 3.1 ^{14}C age
574 calibration program. Radiocarbon 35, 215–230.
575 Stuiver, M., Reimer, P.J., Bard, E., Beck, J.W., Burr, G.S., Hughen, K.A., Kromer, B.,
576 McCormac, G., Van der Plicht, J., Spurk, M., 1998. INTCAL98 Radiocarbon
577 age calibration. Radiocarbon 40, 1041–1083.
578 Yamamoto, S., Kawamura, K., 2010. Application of urea adduction technique to
579 polluted urban aerosols for the determination of hydrogen isotopic
580 composition of *n*-alkanes. International Journal of Environmental Analytical
581 Chemistry, in press.
582 Yudina, N. V., Savel'eva, A. V., 2008. Hydrocarbons in peat-forming plants at eutrophic
583 bogs in western Siberia. Geochemistry International 46, 77–84.
584 Wang, H., Hong, Y., Zhu, Y., Hong, B., Lin, Q., Xu, H., Leng, X., Mao, X., 2004.
585 Humification degrees of peat in Qinghai-Xizang Plateau and palaeoclimate
586 change. Chinese Science Bulletin 49, 514–519.
587 Wang, L., Sarnthein, M., Erlenkeuser, H., Grootes, P. M., Grimalt, J. O., Pelejero, C.,
588 Linck, G., 1999. Holocene variations in Asian monsoon moisture: a bidecadal
589 sediment record from the South China Sea. Geophysical Research Letters 26,
590 2889–2892.

591 Xie, S., Nott, C. J., Avsejs, L. A., Maddy, D., Chambers, F. M., Evershed, R. P., 2004.
592 Molecular and isotopic stratigraphy in an ombrotrophic mire for paleoclimate
593 reconstruction. Geochimica et Cosmochimica Acta 68, 2849–2862.
594 Xu , H., Hong, Y., Lin, Q., Zhu, Y., Hong, B., Jiang, H., 2006. Temperature responses to
595 quasi-100-yr solar variability during the past 6000 years based on $\delta^{18}O$ of peat
596 cellulose in Hongyuan, eastern Qinghai–Tibet plateau, China.
597 Palaeogeography, Palaeoclimatology, Palaeoecology 230, 155–164.
598 Zheng, Y., Zhou, W., Meyers, P. A., Xie, S., 2007. Lipid biomarkers in the
599 Zoigê-Hongyuan peat deposit: Indicators of Holocene climate changes in West
600 China. Organic Geochemistry 38, 1927–1940.
601 Zhou, W., Xie, S., Meyers, P. A., Zheng, Y., 2005. Reconstruction of late glacial and
602 Holocene climate evolution in southern China from geolipids and pollen in the
603 Dingnan peat sequence. Organic Geochemistry 36, 1272–1284.
604 Zhou, W., Zheng, Y., Meyers, P. A., Jull, A. J. T., Xie, S., 2010. Postglacial
605 climate-change record in biomarker lipid compositions of the Hani peat
606 sequence, northeastern China. Earth and Planetary Science Letters 294, 37–46.
607

Table 1
Summary of dominant *n*-alkane homologues in modern plant taxa found at Hani peatland

Plant species (Hong et al., 2005)		Dominant *n*-alkane homologues	References
Sphagnum	*palustre*	C23>C25	Nott et al. (2000), Baas et al. (2000)
S.	*magellamicum*	C31>C25>C29, C25	Nott et al. (2000), Baas et al. (2000)
S.	*acutifolium*		
Polytrichum	*commune*	C31>C29>C33[a]	Nott et al. (2000)
Calliergonella	*cuspidata*		
Eriphorum	*vaginatum*	C31>C33>C29	Nott et al. (2000)
Carex	*schmidtii*	C31>C33>C29[a]	Nichols et al. (2006)
C.	*tenuiflora*		
Phragmitex	*communis*		
Typha	*latifolia*	C29>C27	Cranwell (1984)
Equisetum	*heleocharis*		
Comarum	*palustre*		
Larix	*olgensis*	C31[a]	Maffei et al. (2004)
Betula	*ovalifolia*	C27, C31[a]	Sachse et al. (2006)
Vaccinium	*uliginosum*	C29>C31>C27[a]	Nott et al. (2000)
Ledum	*palustre var. dilatatum*		
L.	*palustre var. angustum*		
Chamaedaphne	*calyculata*	C29>C31	Nichols et al. (2006)

[a] Data adapted from different or unspecified species within the same genera.

609 **Figure captions**

610

611 **Fig. 1.** Map showing the location of the Hani peat bog, northeast China.

612

613 **Fig. 2.** Stratigraphic section of the Hani peat sequence with chronology and histograms
614 of distributions of *n*-alkanes. Note that *n*-alkane distribution in the lower part of the
615 column exhibits important contributions of mid-chain components from mosses. Cal
616 ages are obtained from accelerator mass spectrometry (AMS) ^{14}C ages that were
617 provided by Zhou et al. (2010).

618

619 **Fig. 3.** Depth profiles of carbon isotope ratios ($\delta^{13}C$) of C_{21} to C_{33} odd carbon number
620 *n*-alkanes.

621

622 **Fig. 4.** Profiles of (a), (b) the $\delta^{13}C$ offsets ($\Delta\delta^{13}C$) between the C_{31} *n*-alkane and the C_{21},
623 C_{23}, C_{25}, C_{27}, C_{29} and C_{33} *n*-alkanes, (c), (d) the concentration ratios of the C_{21} to C_{29} odd
624 carbon number *n*-alkanes and the C_{33} *n*-alkane against the C_{31} *n*-alkane, and (e), (f) the
625 P*aq* and the δD of the C_{27} *n*-alkane (Seki et al., 2009) over the last 16 ka. Shaded bands
626 indicate the intervals where the $\Delta\delta^{13}C$ offsets show concomitant variations with the
627 *n*-alkane ratios.

628

629 **Fig. 5.** Variations of (a) the $\delta^{13}C$ of terrestrial higher plant-derived *n*-alkanes (C_{29} and
630 C_{31} *n*-alkanes), (b) the ACL, and (c) the $\delta^{18}O$ (Hong et al., 2009a) and (d) $\delta^{13}C$ of peat
631 cellulose (Hong et al., 2005) in the Hani peat bog. The $\delta^{13}C$ of C_{29} and C_{31} *n*-alkanes and
632 the ACL show parallel fluctuations in a light gray shaded sequence with minimal values
633 at 10.5–9.3 ka and 8.1 ka (dark gray bands).

634

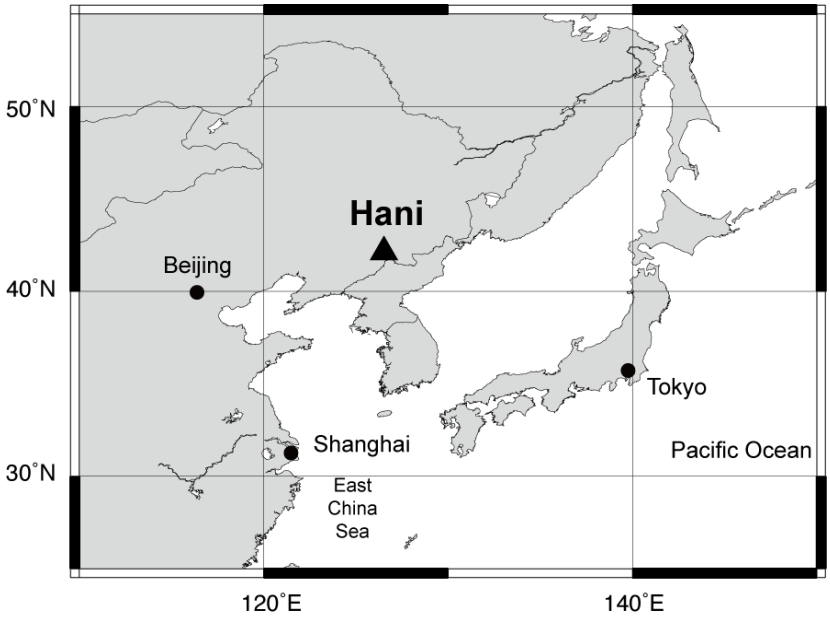

634

635

636 Fig. 1

637

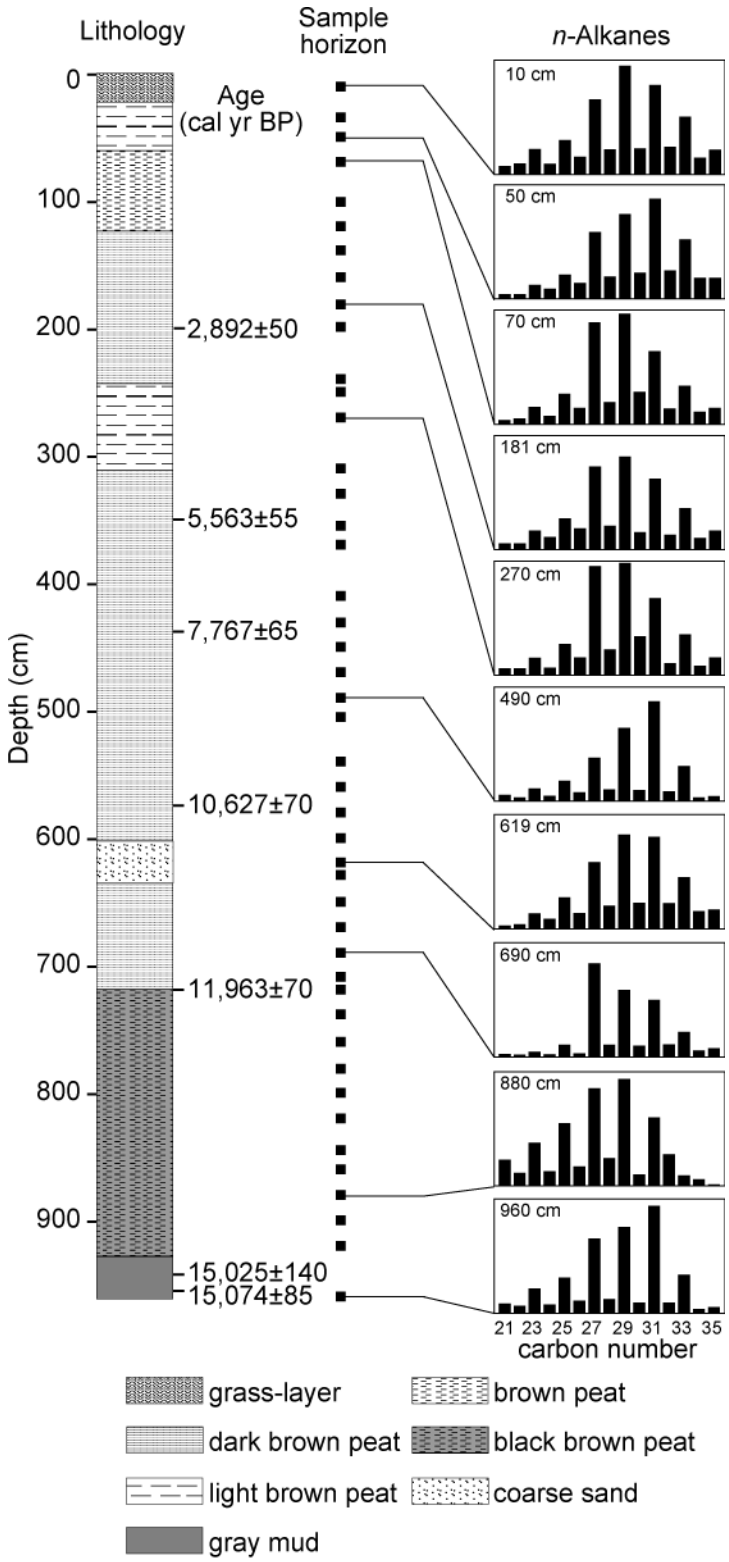

637
638
639 Fig. 2
640

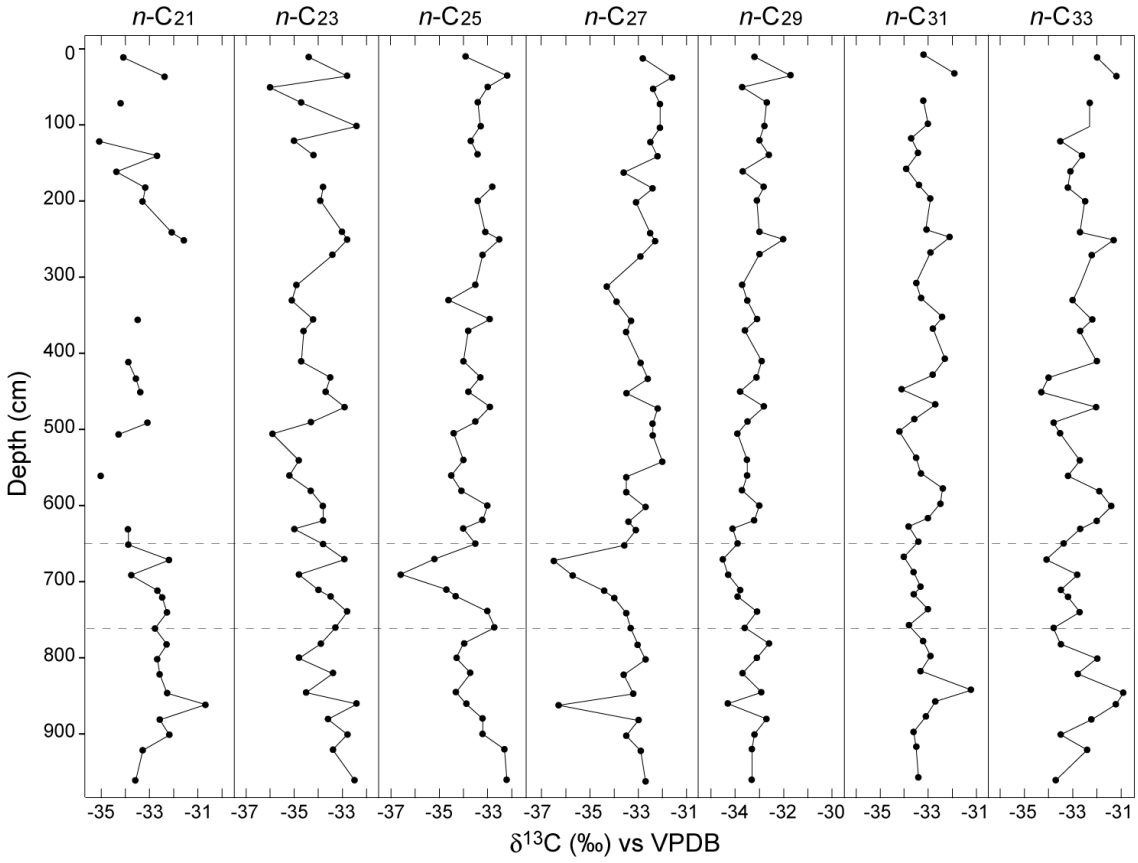

640

641

642 Fig. 3

643

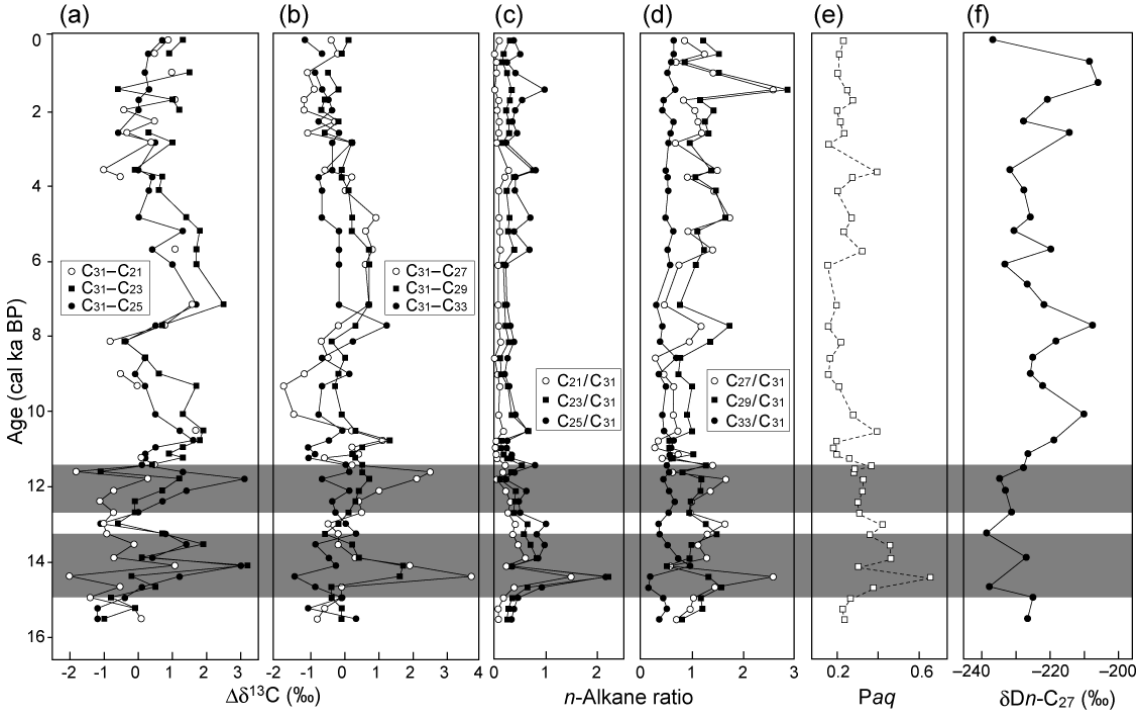

643

644

645 Fig. 4

646

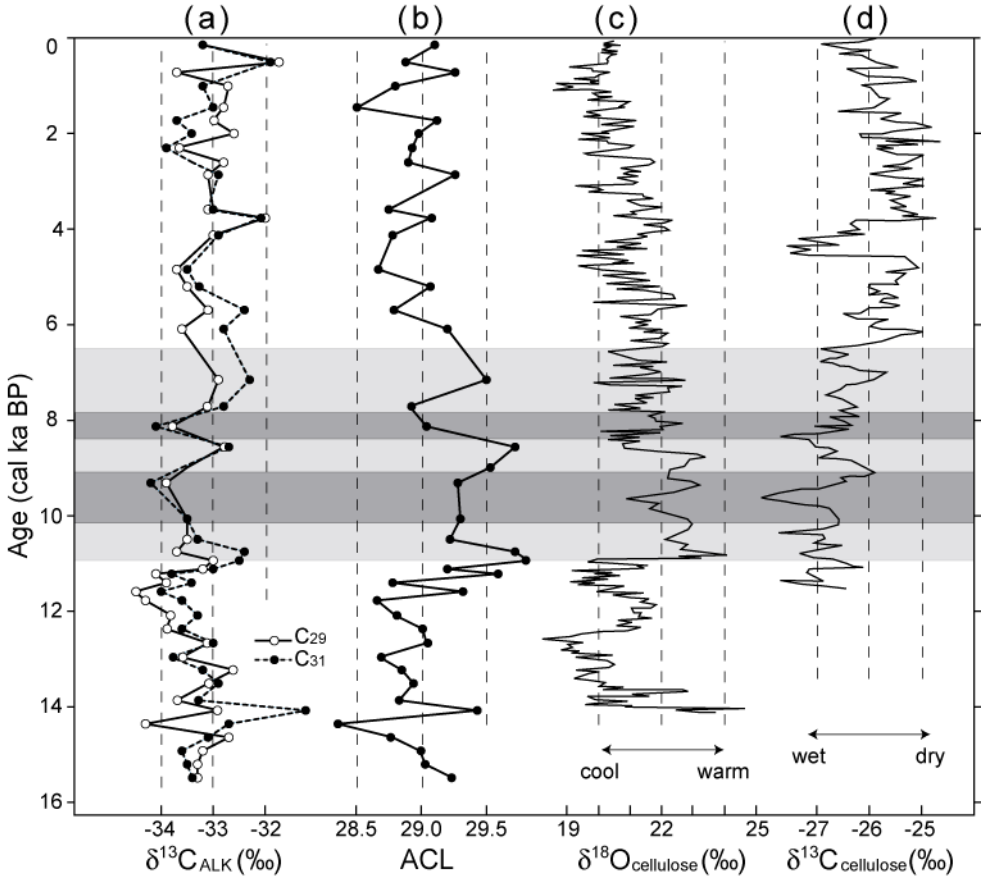

646

647

648 Fig. 5